PRL-TH-95/17
hep-ph/9509299

Decay-lepton angular distribution in polarized $e^+e^- \to t\bar{t}$ and CP-violating dipole couplings of the top quark

P. Poulose and Saurabh D. Rindani

Theory Group, Physical Research Laboratory
Navrangpura, Ahmedabad 380009, India

Abstract

In the presence of an electric dipole coupling of $t\bar{t}$ to a photon, and an analogous "weak" dipole coupling to the Z, CP violation in the process $e^+e^- \to t\bar{t}$ leads to the polarization of the top and anti-top. This polarization can be analyzed by studying the energy and angular distributions of a decay charged lepton (anti-lepton) when the top (anti-top) decays leptonically. We have obtained analytic expressions for these distributions when either t or $\bar{t}$ decays leptonically. We study two types of simple CP-violating angular asymmetries which do not need the full reconstruction of the t or $\bar{t}$. These together can help to determine the electric and weak dipole form factors independently. We have also shown how the use of longitudinal beam polarization can help to do this with only one asymmetry measurement, and to improve the sensitivity.

1 Introduction

Experiments at the Tevatron have seen evidence for the top qark with mass in the range of about 170-200 GeV [1]. Future runs of the experiment will be able to determine the mass more precisely and also determine other properties of the top quark. $t\bar{t}$ pairs will be produced more copiously at proposed e^+e^- linear colliders operating above threshold. It would then be possible to investigate these properties further.

While the standard model (SM) predicts CP violation outside the K-, D- and B-meson systems to be unobservably small, in some extensions of SM, CP violation might be considerably enhanced, especially in the presence of a heavy top quark. In particular, CP-violating electric dipole form factor of the top quark, and the analogous CP-violating "weak" dipole form factor in the $t\bar{t}$ coupling to Z, could be enhanced. These CP-violating form factors could be determined in a model-independent way at high energy e^+e^- linear colliders, where $e^+e^- \to t\bar{t}$ would proceed through virtual γ and Z exchange.

Since a heavy top quark ($m_t \geq 120$ GeV) is expected to decay before it hadronizes [2], it has been suggested [3] that top polarization asymmetry in $e^+e^- \to t\bar{t}$ can be used to determine the CP-violating dipole form factors, since polarization information would be retained in the decay product distribution. Experiments have been proposed in which the CP-violating dipole couplings could be measured in decay momentum correlations [4, 5, 6] or asymmetries [7, 8], even with beam polarization [5, 8]. These suggestions on the measurement of asymmetries have concentrated on experiments requiring the reconstruction of the top-quark momentum (with the exception of lepton energy asymmetry [3, 7, 8]). In this note we look at very simple lepton angular asymmetries which do not require the experimental determination of the t or $\bar{t}$ momentum. Being single-lepton asymmetries, they do not require both t and $\bar{t}$ to decay leptonically. Since either t or $\bar{t}$ is also allowed to decay hadronically, there is a gain in statistics.

Our results are based on fully analytical calculation of single lepton distributions in the production and subsequent decay of $t\bar{t}$. We present fully differential distribution as well as the distribution in the polar angle of the lepton with respect to the beam direction in the centre-of-mass (cm) frame. These distributions in the absence of CP-violating dipole couplings were obtained earlier by Arens and Sehgal [9], using the technique of Kawasaki, Shirafuji and Tsai [10]. We have included CP-violating effects in $t\bar{t}$ produc-

tion, and obtained the distributions using the equivalent helicity-amplitude technique. Our results agree with the results of [9] in the limit of vanishing dipole moments.

We have also included the effect of electron longitudinal polarization, likely to be easily available at linear colliders. In an earlier paper [8], we had shown how polarization helps to put independent limits on electric and weak dipole couplings, while providing greater sensitivity in the case of asymmetries. We also demonstrate these advantages for the present case, strengthening the case for polarization studies.

The rest of the paper is organized as follows. In Sec. II, we describe the calculation of the decay-lepton angular distribution from a decaying t or $\overline{t}$ in $e^+e^- \to t\overline{t}$. In Sec. III we describe CP-violating asymmetries and obtain expressions for them. Numerical results are presented in Sec. IV, and Sec. V contains our conclusions. The Appendix contains certain expressions which are too lengthy to be put in the main text.

2 Calculation of lepton angular distributions

We describe in this Section the calculation of l^+ (l^-) distribution in $e^+e^- \to t\overline{t}$ and the subsequent decay $t \to bl^+\nu_l$ ($\overline{t} \to \overline{b}l^-\overline{\nu_l}$). We adopt the narrow-width approximation for t and $\overline{t}$, as well as for $W^\pm$ produced in t, $\overline{t}$ decay.

We assume the top quark couplings to γ and Z to be given by the vertex factor $ie\Gamma^j_\mu$, where

$$\Gamma^j_\mu \;=\; c^j_v\,\gamma_\mu \;+\; c^j_a\,\gamma_\mu\,\gamma_5 \;+\; \frac{c^j_d}{2\,m_t}\,i\gamma_5\,(p_t \;-\; p_{\overline{t}})_\mu, \;\; j \;=\; \gamma, Z, \tag{1}$$

with

$$\begin{aligned} c^\gamma_v &= \frac{2}{3}, \quad c^\gamma_a \;=\; 0, \\ c^Z_d &= \frac{\left(\frac{1}{4} - \frac{2}{3}\,x_w\right)}{\sqrt{x_w\,(1-x_w)}}, \\ c^Z_a &= -\frac{1}{4\sqrt{x_w\,(1-x_w)}}, \end{aligned} \tag{2}$$

and $x_w = sin^2\theta_w$, θ_w being the weak mixing angle. We have assumed in (1) that the only addition to the SM couplings $c_{v,a}^{\gamma,Z}$ are the CP-violating electric and weak dipole form factors, ec_d^γ/m_t and ec_d^Z/m_t, which are assumed small. Use has also been made of the Dirac equation in rewriting the usual dipole coupling $\sigma_{\mu\nu}(p_t + p_{\overline{t}})^\nu\gamma_5$ as $i\gamma_5(p_t - p_{\overline{t}})_\mu$, dropping small corrections to the vector and axial-vector couplings. We assume that there is no CP violation in t, $\overline{t}$ decay [11].

The helicity amplitudes for $e^+e^- \to \gamma^*, Z^* \to t\overline{t}$ in the cm frame, including $c_d^{\gamma,Z}$ couplings, have been given in [7] (see also Kane *et al.*, ref. [3]), so we do not repeat them here. The non-vanishing helicity amplitudes, respectively M and $\overline{M}$, for

$$t \to bW^+, \;\; W^+ \to l^+\nu_l$$

and

$$\overline{t} \to \overline{b}W^-, \;\; W^- \to l^-\overline{\nu_l}$$

in the respective rest frames of t, $\overline{t}$, are given below (we assume standard model couplings and neglect all masses except m_t, the top mass):

$$M_{+-+-} = 8g^2\Delta_W(q)\cos\frac{\theta_{l^+}}{2}\left[\cos\frac{\theta_{\nu_l}}{2}\sin\frac{\theta_b}{2}e^{-i\phi_b} - \sin\frac{\theta_{\nu_l}}{2}\cos\frac{\theta_b}{2}e^{-i\phi_{\nu_l}}\right]e^{i\phi_{l^+}}, \tag{3}$$

$$M_{--+-} = 8g^2\Delta_W(q)\sin\frac{\theta_{l^+}}{2}\left[\cos\frac{\theta_{\nu_l}}{2}\sin\frac{\theta_b}{2}e^{-i\phi_b} - \sin\frac{\theta_{\nu_l}}{2}\cos\frac{\theta_b}{2}e^{-i\phi_{\nu_l}}\right], \tag{4}$$

$$\overline{M}_{++-+} = 8g^2\Delta_W(q)\cos\frac{\theta_{l^-}}{2}\left[\cos\frac{\theta_{\overline{\nu_l}}}{2}\sin\frac{\theta_{\overline{b}}}{2}e^{i\phi_{\overline{\nu_l}}} - \sin\frac{\theta_{\overline{\nu_l}}}{2}\cos\frac{\theta_{\overline{b}}}{2}e^{i\phi_{\overline{b}}}\right], \tag{5}$$

$$\overline{M}_{-+-+} = 8g^2\Delta_W(q)\sin\frac{\theta_{l^-}}{2}\left[\cos\frac{\theta_{\overline{\nu_l}}}{2}\sin\frac{\theta_{\overline{b}}}{2}e^{i\phi_{\overline{\nu_l}}} - \sin\frac{\theta_{\overline{\nu_l}}}{2}\cos\frac{\theta_{\overline{b}}}{2}e^{i\phi_{\overline{b}}}\right]e^{-i\phi_{l^-}}, \tag{6}$$

where

$$\Delta_W(q) = \frac{1}{q^2 - m_W^2 + i\Gamma_W m_W} \tag{7}$$

is the W propagator, q being the total e^+e^- momentum. The subscripts $\pm$ refer to signs of the helicities, the order of the helicities being t, b, l^+, ν_l ($\overline{t}$, $\overline{b}$, l^-, $\overline{\nu_l}$). The various θ's are polar angles of the particles and antiparticles labelled by the suffixes with respect to a z axis in the direction in which

the top momentum is boosted to go to the cm frame. ϕ's are the azimuthal angles with respect to an x axis chosen in the plane containing the e^- and t directions.

Combining the production and decay amplitudes in the narrow-width approximation for $t, \overline{t}, W^+, W^-$, and using appropriate Lorentz boosts to calculate everything in the e^+e^- cm frame, we get the l^+ and l^- distributions for the case of e^-, e^+ with polarization P_e, $P_{\overline{e}}$ to be:

$$\begin{aligned}
\frac{d\sigma^{\pm}}{d\cos\theta_t dE_l d\cos\theta_l d\phi_l} &= \frac{3\alpha^4\beta}{16x_w^2\sqrt{s}}\frac{E_l}{\Gamma_t\Gamma_W m_W}\left(\frac{1}{1-\beta\cos\theta_{tl}} - \frac{4E_l}{\sqrt{s}(1-\beta^2)}\right) \\
&\times\Big\{\Big(A_0 + A_1\cos\theta_t + A_2\cos^2\theta_t\Big)(1-\beta\cos\theta_{tl}) \\
&+\Big(B_0^{\pm} + B_1\cos\theta_t + B_2^{\pm}\cos^2\theta_t\Big)(\cos\theta_{tl}-\beta) \\
&+\Big(C_0^{\pm} + C_1^{\pm}\cos\theta_t\Big)(1-\beta^2)\sin\theta_t\sin\theta_l(\cos\theta_t\cos\phi_l - \sin\theta_t\cot\theta_l) \\
&+\Big(D_0^{\pm} + D_1^{\pm}\cos\theta_t\Big)(1-\beta^2)\sin\theta_t\sin\theta_l\sin\phi_l\Big\}. \qquad (8)
\end{aligned}$$

The quantities A_i, B_i, C_i and D_i occurring in the above equation are functions of the masses, s, the degrees of e and $\overline{e}$ polarization (P_e and $P_{\overline{e}}$), and the coupling constants. They are listed in the Appendix.

In eq. (8), σ^+ and σ^- refer respectively to l^+ and l^- distributions, with the same notation for the kinematic variables of particles and antiparticles. Thus, θ_t, is the polar angle of t (or $\overline{t}$), and E_l, θ_l, ϕ_l are the energy, polar angle and azimuthal angle of l^+ (or l^-). All the angles are now in the cm frame, with the z axis chosen along the e^- momentum, and the x axis chosen in the plane containing the e^- and t directions. θ_{tl} is the angle between the t and l^+ directions (or $\overline{t}$ and l^- directions). β is the t (or $\overline{t}$) velocity: $\beta = \sqrt{1-4m_t^2/s}$, and $\gamma = 1/\sqrt{1-\beta^2}$.

Since we are mainly interested in θ_l distributions here, we first integrate over E_l between limits

$$\frac{m_W^2}{m_t^2}\frac{\sqrt{s}}{4}\frac{1-\beta^2}{1-\beta\cos\theta_{tl}} \;<\; E_l \;<\; \frac{\sqrt{s}}{4}\frac{1-\beta^2}{1-\beta\cos\theta_{tl}},$$

then over ϕ from 0 to 2π, and finally over $\cos\theta_t$ from -1 to $+1$. After some lengthy algebra, we get the final result as

$$\frac{d\sigma^{\pm}}{d\cos\theta_l} \;=\; \frac{3\pi\alpha^2}{32s}B_t B_{\overline{t}}\left\{4A_0 - 2A_1\left(\frac{1-\beta^2}{\beta^2}\log\frac{1+\beta}{1-\beta} - \frac{2}{\beta}\right)\cos\theta_l\right.$$

$$
\begin{aligned}
&+2A_2\left(\frac{1-\beta^2}{\beta^3}\log\frac{1+\beta}{1-\beta}(1-3\cos^2\theta_l)\right.\\
&\left.-\frac{2}{\beta^2}(1-3\cos^2\theta_l-\beta^2+2\beta^2\cos^2\theta_l)\right)\\
&+2B_1\frac{1-\beta^2}{\beta^2}\left(\frac{1}{\beta}\log\frac{1-\beta}{1-\beta}-2\right)\cos\theta_l\\
&+B_2^{\pm}\frac{1}{\beta^3}\left(\frac{\beta^2-2}{\beta}\log\frac{1+\beta}{1-\beta}+6\right)(1-3\cos^2\theta_l)\\
&+2C_0^{\pm}\frac{1-\beta^2}{\beta^2}\left(\frac{1}{\beta}\log\frac{1+\beta}{1-\beta}-2\right)\cos\theta_l\\
&\left.-C_1^{\pm}\frac{1}{\beta^3}\left(\frac{3(1-\beta^2)}{\beta}\log\frac{1+\beta}{1-\beta}-2(3-2\beta^2)\right)(1-3\cos^2\theta_l)\right\},
\end{aligned}
\tag{9}
$$

where B_t and $B_{\overline{t}}$ are respectively the branching ratios of t and $\overline{t}$ into the final states being considered.

We have compared our expression for the angular distribution with the one in [9] in the limit of vanishing dipole moments and vanishing beam polarization, and found agreement.

3 CP-violating angular asymmetries

We define two independent CP-violating asymmetries, which depend on different linear combinations of $\mathrm{Im}c_d^\gamma$ and $\mathrm{Im}c_d^Z$. (It is not possible to define CP-odd quantities which determine $\mathrm{Re}c_d^{\gamma,Z}$ using single-lepton distributions, as can be seen from the expression for the CP-odd combination $\frac{d\sigma^+}{d\cos\theta_l}(\theta_l)-\frac{d\sigma^-}{d\cos\theta_l}(\pi-\theta_l)$). One is simply the total lepton-charge asymmetry, with a cut-off of θ_0 on the forward and backward directions:

$$
\mathcal{A}_{ch}(\theta_0)=\frac{\displaystyle\int_{\theta_0}^{\pi-\theta_0}d\theta_l\left(\frac{d\sigma^+}{d\theta_l}-\frac{d\sigma^-}{d\theta_l}\right)}{\displaystyle\int_{\theta_0}^{\pi-\theta_0}d\theta_l\left(\frac{d\sigma^+}{d\theta_l}+\frac{d\sigma^-}{d\theta_l}\right)}. \tag{10}
$$

The other is the leptonic forward-backward asymmetry combined with charge asymmetry, again with the angles within θ_0 of the forward and backward

directions excluded:

$$\mathcal{A}_{fb}(\theta_0) = \frac{\int_{\theta_0}^{\frac{\pi}{2}} d\theta_l \left(\frac{d\sigma^+}{d\theta_l} - \frac{d\sigma^-}{d\theta_l}\right) - \int_{\frac{\pi}{2}}^{\pi-\theta_0} d\theta_l \left(\frac{d\sigma^+}{d\theta_l} - \frac{d\sigma^-}{d\theta_l}\right)}{\int_{\theta_0}^{\pi-\theta_0} d\theta_l \left(\frac{d\sigma^+}{d\theta_l} + \frac{d\sigma^-}{d\theta_l}\right)}. \qquad (11)$$

These asymmetries are a measure of CP violation in the unpolarized case and in the case when polarization is present, but $P_e = -P_{\overline{e}}$. When $P_e \neq -P_{\overline{e}}$, the initial state is not invariant under CP, and therefore CP-invariant interactions can contribute to the asymmetries. However, to the leading order in α, these CP-invariant contributions vanish in the limit $m_e = 0$. Order-α collinear helicity-flip photon emission can give a CP-even contribution. However, this background can be suppressed by a suitable cut on the visible energy.

The expressions for $\mathcal{A}_{ch}(\theta_0)$ and $\mathcal{A}_{fb}(\theta_0)$ may be derived from eq. (9) making use of the expressions in the Appendix, and are given below.

$$\begin{aligned}\mathcal{A}_{ch}(\theta_0) = {} & \frac{1}{2\sigma(\theta_0)} \frac{3\pi\alpha^2}{4s} B_t B_{\overline{t}}\, 2\cos\theta_0 \sin^2\theta_0 \left((1-\beta^2)\log\frac{1+\beta}{1-\beta} - 2\beta\right) \\ & \times \Big(\mathrm{Im}c_d^\gamma \Big\{\Big[2c_v^\gamma + (r_L + r_R)c_v^Z\Big](1 - P_e P_{\overline{e}}) + (r_L - r_R)c_v^Z(P_{\overline{e}} - P_e)\Big\} \\ & + \mathrm{Im}c_d^Z \Big\{\Big[(r_L + r_R)c_v^\gamma + (r_L^2 + r_R^2)c_v^Z\Big](1 - P_e P_{\overline{e}}) + [(r_L - r_R)c_v^\gamma \\ & + (r_L^2 - r_R^2)c_v^Z\Big](P_{\overline{e}} - P_e)\Big\}\Big); \end{aligned} \qquad (12)$$

$$\begin{aligned}\mathcal{A}_{fb}(\theta_0) = {} & \frac{1}{2\sigma(\theta_0)} \frac{3\pi\alpha^2}{2s} B_t B_{\overline{t}} \cos^2\theta_0 \left((1-\beta^2)\log\frac{1+\beta}{1-\beta} - 2\beta\right) c_a^Z \\ & \times \{\mathrm{Im}c_d^\gamma [(r_L - r_R)(1 - P_e P_{\overline{e}}) + (r_L + r_R)(P_{\overline{e}} - P_e)] \\ & + \mathrm{Im}c_d^Z \left[(r_L^2 - r_R^2)(1 - P_e P_{\overline{e}}) + (r_L^2 + r_R^2)(P_{\overline{e}} - P_e)\right]\}. \end{aligned} \qquad (13)$$

Here $\sigma(\theta_0)$ is the cross section for l^+ or l^- production with a cut-off θ_0, and is given by

$$\begin{aligned}\sigma(\theta_0) = {} & \frac{3\pi\alpha^2}{8s} B_t B_{\overline{t}}\, 2\cos\theta_0 \left(\left\{(1-\beta^2)\log\frac{1+\beta}{1-\beta}\sin^2\theta_0\right.\right. \\ & \left.\left. + 2\beta\left[1 + (1 - \frac{2}{3}\beta^2)\cos^2\theta_0\right]\right\}\right.\end{aligned}$$

$$
\begin{aligned}
&\times \left\{ \left[2c_v^{\gamma 2} + 2c_v^\gamma c_v^Z (r_L + r_R) + c_v^{Z^2} (r_L^2 + r_R^2) \right] (1 - P_e P_{\overline{e}}) \right. \\
&\left. + c_v^Z \left[(r_L - r_R) c_v^\gamma + (r_L^2 - r_R^2) c_v^Z \right] (P_{\overline{e}} - P_e) \right\} \\
&+ \left\{ (1 - \beta^2) \log \frac{1+\beta}{1-\beta} \sin^2 \theta_0 + 2\beta \left[2\beta^2 - 1 + (1 - \frac{2}{3}\beta^2) \cos^2 \theta_0 \right] \right\} \\
&\times c_a^{Z^2} \left\{ (r_L^2 + r_R^2)(1 - P_e P_{\overline{e}}) + (r_L^2 - r_R^2)(P_{\overline{e}} - P_e) \right\} - 2(1 - \beta^2) \\
&\times \left(\log \frac{1+\beta}{1-\beta} - 2 \right) \sin^2 \theta_0 c_a^Z \left\{ \left[(r_L + r_R) c_v^\gamma + (r_L^2 + r_R^2) c_v^Z \right] \right. \\
&\left. \times \ (1 - P_e P_{\overline{e}}) + \left[(r_L - r_R) c_v^\gamma + (r_L^2 - r_R^2) c_v^Z \right] (P_{\overline{e}} - P_e) \right\} \Big) . \qquad (14)
\end{aligned}
$$

We note the curious fact that $\mathcal{A}_{ch}(\theta_0)$ vanishes for $\theta_0 = 0$. This implies that the CP-violating charge asymmetry does not exist unless a cut-off is imposed on the lepton production angle. $\mathcal{A}_{fb}(\theta_0)$, however, is nonzero for $\theta_0 = 0$.

It is also possible to obtain a variety of CP-odd correlations using the analytic form (9). However, we restrict ourselves here to an analysis of the consequences of $\mathcal{A}_{ch}$ and $\mathcal{A}_{fb}$, without and with beam polarization.

4 Numerical Results

In this section we describe the numerical results for the calculation of 90% confidence level (CL) limits that could be put on $\mathrm{Im}c_d^{\gamma,Z}$ using the asymmetries described in the previous sections, as well as the CP-odd part of the angular distribution in eq. (9).

We look at only semileptonic final states. That is to say, when t decays leptonically, we assume $\overline{t}$ decays hadronically, and *vice versa*. We sum over the electron and muon decay channels. Thus, $B_t B_{\overline{t}}$ is taken to be $2/3 \times 2/9$. The number of events for various relevant θ_0 and for beam polarizations $P_e = 0, \pm 0.5$ are listed in Table 1.

In each case we have derived simultaneous 90% CL limits on $\mathrm{Im}c_d^\gamma$ and $\mathrm{Im}c_d^Z$ that could be put in an experiment at a future linear colider with $\sqrt{s} = 500$ GeV and an integrated luminosity of 10 fb^{-1}. We do this by equating the asymmetry ($\mathcal{A}_{ch}$ or $\mathcal{A}_{fb}$) to $2.15/\sqrt{N}$, where N is the total number of expected events. In the unpolarized case, each of $\mathcal{A}_{ch}$ and $\mathcal{A}_{fb}$ gives a band of allowed values in the $\mathrm{Im}c_d^\gamma$–$\mathrm{Im}c_d^Z$ plane. If both $\mathcal{A}_{ch}$ and $\mathcal{A}_{fb}$

are looked for in an experiment, the intersection region of the corresponding bands determines the best 90% CL limits which can be put simultaneously on $\mathrm{Im}c_d^\gamma$ and $\mathrm{Im}c_d^Z$. These best results are obtained for $\theta_0 = 35^\circ$ and are shown in Fig. 1(a) and Fig. 1(b), for two values of the top mass, $m_t = 174$ GeV, and $m_t = 200$ GeV respectively.

We see from Fig. 1 that the 90% CL limits that could be put on $\mathrm{Im}c_d^\gamma$ and $\mathrm{Im}c_d^Z$ simultaneously are, respectively, 2.4 and 17, for $m_t = 174$ GeV. The same limits are 4.0 and 28 for $m_t = 200$ GeV.

In the case where the e^- beam is longitudinally polarized, we have assumed the degree of polarization $P_e = \pm 0.5$, and determined 90% CL limits which can be achieved. In this case, the use of $P_e = +0.5$ and $P_e = -0.5$ is sufficient to constrain $\mathrm{Im}c_d^\gamma$ and $\mathrm{Im}c_d^Z$ simultaneously even though only one asymmetry (either $\mathcal{A}_{ch}$ or $\mathcal{A}_{fb}$) is determined. The 90% CL bands corresponding to $P_e = \pm 0.5$ are shown in Figs. 2 and 3, for $\mathcal{A}_{ch}$ with $\theta_0 = 60^\circ$, and for $\mathcal{A}_{fb}$ with $\theta_0 = 10^\circ$, respectively. Again, these values of θ_0 are chosen to maximize the sensitivity [12].

It can be seen from these figures that the simultaneous limits expected to be obtained on $\mathrm{Im}c_d^\gamma$ and $\mathrm{Im}c_d^Z$ are, respectively, about 0.45 and 1.5 for $m_t = 174$ GeV from both the types of asymmetries. These limits are about 0.78 and 2.5 for $m_t = 200$ GeV. We see thus that the use of polarization leads to an improvement of by a factor of about 5 in the sensitivity to the measurement of $\mathrm{Im}c_d^\gamma$, and by a factor of at least 10 in the case of $\mathrm{Im}c_d^Z$. Moreover, with polarization, either of $\mathcal{A}_{fb}$ and $\mathcal{A}_{ch}$, with a suitably chosen cut-off, suffices to get the same improvement in sensitivity.

Apart from simultaneous limits on $\mathrm{Im}c_d^{\gamma,Z}$, we have also found out the sensitivities of one of $\mathrm{Im}c_d^{\gamma,Z}$, assuming the other to be zero, using the CP-odd combination of angular distributions $\frac{d\sigma^+}{d\cos\theta}(\theta_l) - \frac{d\sigma^-}{d\cos\theta}(\pi - \theta_l)$ coming from eq. (19). We assume that the data is collected over bins in θ_l, and add the 90% CL limits obtained from individual bins in inverse quadrature. We find that the best individual limits are respectively 0.12 and 0.28 for $\mathrm{Im}c_d^\gamma$ and $\mathrm{Im}c_d^Z$, both in the case of $P_e = -0.5$, for $m_t = 174$ GeV. The corresponding limits for $m_t = 200$ GeV are 0.18 and 0.43. As expected, these limits are better than simultaneous ones. Even here, there is an improvement due to polarization, but it is not as dramatic as in the case of simultaneous limits.

Our limits on $\mathrm{Im}c_d^{\gamma,Z}$ are summarized in Table 2.

5 Conclusions

We have calculated analytically the single-lepton angular distribution in the production and subsequent decay of $t\overline{t}$ in the presence of electric and weak dipole form factors of the top quark. We have included effects of longitudinal beam polarization. We have then obtained expressions for certain simple CP-violating angular asymmetries, specially chosen so that they do not require the reconstruction of the t or $\overline{t}$ directions or energies. We have analyzed these asymmetries to obtain simultaneous 90% CL limits on the imaginary parts of the electric and weak dipole couplings which would be possible at future linear e^+e^- collider operating at $\sqrt{s} = 500$ GeV and with a luminosity of 10 fb^{-1}. Figs. 1-3 show the allowed regions in the Imc_d^γ–Imc_d^Z plane at the 90% CL. Table 2 summarizes the 90% CL limits on Im$c_d^{\gamma,Z}$ in various cases.

Our general conclusion is that the sensitivity to the measurement of dipole couplings is improved considerably if the electron beam is polarized, a situation which might easily obtain at linear colliders. Another general observation is that the sensitivity is better for a lower top mass than a higher one.

If we compare these results for sensitivities with those obtained in [8], where we studied asymmetries requiring the top momentum determination, we find that while the sensitivities with the asymmetries studied here are worse by a factor of about 3 in the unpolarized case, the limits in the polarized case are higher by a factor of about 2 as compared to the those in [8]. It is likely that since in the experiments suggested here, only the lepton momenta need be measured, improvement in experimental accuracy can easily compensate for these factors. A detailed simulation of experimental conditions is needed to reach a definite conclusion on the exact overall sensitivities.

We have also compared our results with those of [6], where CP-odd momentum correlations are studied in the presence of e^- polarization. With comparable parameters, the sensitivities we obtain are comparable to those obtained in [6]. In some cases our sensitivities are slightly worse because we require either t or $\overline{t}$ to decay leptonically, leading to a reduced event rate. However, the better experimental efficiencies in lepton momentum measurement may again compensate for this loss.

As mentioned earlier, since we consider only the electron beam to be polarized, the asymmetries considered here can have backgrounds from order-α collinear initial-state photon emission, which, in principle, have to be cal-

culated and subtracted. However, in case of correlations, it was found in [13] that the background contribution can be neglected for the luminosity we assume here. This is likely to be the case in the asymmetries we consider here.

The theoretical predictions for $c_d^{\gamma,Z}$ are at the level of $10^{-2} - 10^{-3}$, as for example, in the Higgs-exchange and supersymmetric models of CP violation [4, 7, 14]. Hence the measurements suggested here cannot exclude these modes at the 90% C.L. However, as simultaneous model-independent limits on both c_d^Z and c_d^γ, the ones obtainable from the experiments we suggest, are an improvement over those obtainable from measurements in unpolarized experiments.

Increase in polarization beyond ± 0.5 can increase the asymmetries in some cases we consider. Also, a change in the $e^+ e^-$ cm energy also has an effect on the asymmetries. However, we have tried to give here only the salient features of the outcome of a possible experiment in the presence of longitudinal beam polarization.

Inclusion of experimental detection efficiencies may change our results somewhat. However, the main thrust of our conclusions, that longitudinal beam polarization improves the sensitivity, would still be valid.

Appendix

The expressions for A_i, B_i, C_i and D_i occurring in equation (8) are listed below.

$$
\begin{aligned}
A_0 &= \Big\{2(2-\beta^2)\left[2{c_v^\gamma}^2+2(r_L+r_R)c_v^\gamma c_v^Z+(r_L^2+r_R^2){c_v^Z}^2\right] \\
&\quad +2\beta^2(r_L^2+r_R^2){c_a^Z}^2\Big\}(1-P_eP_{\overline{e}}) \\
&\quad +\Big\{2(2-\beta^2)\left[2(r_L-r_R)c_v^\gamma c_v^Z+(r_L^2-r_R^2){c_v^Z}^2\right] \\
&\quad +2\beta^2(r_L^2-r_R^2){c_a^Z}^2\Big\}(P_{\overline{e}}-P_e), \\
A_1 &= -8\beta c_a^Z\Big\{\left[(r_L-r_R)c_v^\gamma+(r_L^2-r_R^2)c_v^Z\right](1-P_eP_{\overline{e}}) \\
&\quad +\left[(r_L+r_R)c_v^\gamma+(r_L^2+r_R^2)c_v^Z\right](P_{\overline{e}}-P_e)\Big\}, \\
A_2 &= 2\beta^2\Big\{\left[2{c_v^\gamma}^2+2(r_L+r_R)c_v^\gamma c_v^Z+(r_L^2+r_R^2)\left({c_v^Z}^2+{c_a^Z}^2\right)\right](1-P_eP_{\overline{e}}) \\
&\quad +\left[2(r_L-r_R)c_v^\gamma c_v^Z+(r_L^2-r_R^2)\left({c_v^Z}^2+{c_v^Z}^2\right)\right](P_{\overline{e}}-P_e)\Big\}, \\
B_0^\pm &= 4\beta\Big\{\left(c_v^\gamma+r_Lc_v^Z\right)\left(r_Lc_a^Z\mp\mathrm{Im}c_d^\gamma\mp r_L\mathrm{Im}c_d^Z\right)(1-P_e)(1+P_{\overline{e}}) \\
&\quad +\left(c_v^\gamma+r_Rc_v^Z\right)\left(r_Rc_a^Z\mp\mathrm{Im}c_d^\gamma\mp r_R\mathrm{Im}c_d^Z\right)(1+P_e)(1-P_{\overline{e}})\Big\}, \\
B_1 &= -4\Big\{\left[(c_v^\gamma+r_Lc_v^Z)^2+\beta^2r_L^2{c_a^Z}^2\right](1-P_e)(1+P_{\overline{e}}) \\
&\quad -\left[(c_v^\gamma+r_Rc_v^Z)^2+\beta^2r_R^2{c_a^Z}^2\right](1+P_e)(1-P_{\overline{e}})\Big\}, \\
B_2^\pm &= 4\beta\Big\{\left(c_v^\gamma+r_Lc_v^Z\right)\left(r_Lc_a^Z\pm\mathrm{Im}c_d^\gamma\pm r_L\mathrm{Im}c_d^Z\right)(1-P_e)(1+P_{\overline{e}}) \\
&\quad +\left(c_v^\gamma+r_Rc_v^Z\right)\left(r_Rc_a^Z\pm\mathrm{Im}c_d^\gamma\pm r_R\mathrm{Im}c_d^Z\right)(1+P_e)(1-P_{\overline{e}})\Big\}, \\
C_0^\pm &= 4\Big\{\left[(c_v^\gamma+r_Lc_v^Z)^2\pm\beta^2\gamma^2c_a^Z\left(\mathrm{Im}c_d^\gamma r_L+\mathrm{Im}c_d^Zr_L^2\right)\right](1-P_e)(1+P_{\overline{e}}) \\
&\quad -\left[(c_v^\gamma+r_Rc_v^Z)^2\pm\beta^2\gamma^2c_a^Z\left(\mathrm{Im}c_d^\gamma r_R+\mathrm{Im}c_d^Zr_R^2\right)\right](1+P_e)(1-P_{\overline{e}})\Big\}, \\
C_1^\pm &= -4\beta\Big\{\left(c_v^\gamma+r_Lc_v^Z\right)\left(r_Lc_a^Z\pm\gamma^2\mathrm{Im}c_d^\gamma\pm r_L\gamma^2\mathrm{Im}c_d^Z\right)(1-P_e)(1+P_{\overline{e}}) \\
&\quad +\left(c_v^\gamma+r_Rc_v^Z\right)\left(r_Rc_a^Z\pm\gamma^2\mathrm{Im}c_d^\gamma\pm r_R\gamma^2\mathrm{Im}c_d^Z\right)(1+P_e)(1-P_{\overline{e}})\Big\}, \\
D_0^\pm &= \mp4\beta\gamma^2\Big\{\left(c_v^\gamma+r_Lc_v^Z\right)\left(\mathrm{Re}c_d^\gamma+r_L\mathrm{Re}c_d^Z\right)(1-P_e)(1+P_{\overline{e}})
\end{aligned}
$$

$$
\begin{aligned}
& - \left(c_v^\gamma + r_R c_v^Z\right)\left(\mathrm{Re}c_d^\gamma + r_R \mathrm{Re}c_d^Z\right)(1+P_e)(1-P_{\overline{e}})\Big\}\,, \\
D_1^{\pm} &= \pm 4\beta^2 c_a^Z \Big\{ r_L \left(\mathrm{Re}c_d^\gamma + r_L \mathrm{Re}c_d^Z\right)(1-P_e)(1+P_{\overline{e}}) \\
& + r_R \left(\mathrm{Re}c_d^\gamma + r_R \mathrm{Re}c_d^Z\right)(1+P_e)(1-P_{\overline{e}})\Big\}\,.
\end{aligned}
$$

References

[1] F. Abe *et al.* (CDF Collab.), Phys. Rev. Lett. **74**, 2626 (1995); S. Abachi *et al.* (D0 Collab.), Phys. Rev. Lett. **74**, 2632 (1995).

[2] I. Bigi and H. Krasemann, Z. Phys. C **7**, 127 (1981); J. Kühn, Acta Phys. Austr. Suppl. **XXIV**, 203 (1982); I. Bigi *et al.*, Phys. Lett. B **181**, 157 (1986).

[3] J.F. Donoghue and G. Valencia, Phys. Rev. Lett. **58**, 451 (1987); C.A. Nelson, Phys. Rev. D **41**, 2805 (1990); G.L. Kane, G.A. Ladinsky and C.-P. Yuan, Phys. Rev. D **45**, 124 (1991); C.R. Schmidt and M.E. Peskin, Phys. Rev. Lett. **69**, 410 (1992); C.R. Schmidt, Phys. Lett. B **293**, 111 (1992); T. Arens and L.M. Sehgal, Phys. Rev. D **50**, 4372 (1994).

[4] W. Bernreuther, T. Schröder and T.N. Pham, Phys. Lett. B **279**, (1992); W. Bernreuther and P. Overmann, Nucl. Phys. B **388**, 53 (1992); Z. Phys. C **61**, 599 (1994); W. Bernreuther and A. Brandenburg, Phys. Lett. B **314** 104 (1993); Phys. Rev. D **49**, 4481 (1994); J.P. Ma and A. Brandenburg, Z. Phys. C **56**, 97 (1992); A. Brandenburg and J.P. Ma, Phys. Lett. B **298**, 211 (1993).

[5] D. Atwood and A. Soni, Phys. Rev. D **45**, 2405 (1992). This paper introduces optimal variables whose expectation values maximize the statistical sensitivity.

[6] F. Cuypers and S.D. Rindani, Phys. Lett. B **343**, 333 (1994).

[7] D. Chang, W.-Y. Keung and I. Phillips, Nucl. Phys. B **408**, 286 (1993); **429**, 255 (1994) (E).

[8] P. Poulose and S.D. Rindani, Phys. Lett. B **349**, 379 (1995).

[9] T. Arens and L.M. Sehgal, Nucl. Phys. B **393**, 46 (1993).

[10] S.Y. Tsai, Phys. Rev. D **4**, 2821 (1971); S. Kawasaki, T. Shirafuji and S.Y. Tsai, Prog. Theo. Phys. **49**, 1656 (1973).

[11] CP violation in top decays has been considered, for example, in B. Grzadkowski and W.-Y. Keung, Phys. Lett. B 316 (1993) 137; E. Christova and M. Fabbrichesi, Phys. Lett. B **320**, 299 (1994); A. Bartl, E.

Christova and W. Majerotto, Preprint HEPHY-PUB 624/95, UWThPh-1995-9, hepph/9507445 (1995).

[12] In case of $\mathcal{A}_{fb}$, the choice $\theta_0 = 0$ also gives very similar sensitivities. However, since this condition would be impossible to achieve in a practical situation, we choose a nonzero value of θ_0.

[13] B. Ananthanarayan and S.D. Rindani, Phys. Rev. D **52**, 2684 (1995).

[14] A. Bartl *et al.*, ref. [11].

Figure Captions

Fig. 1. Bands showing simultaneous 90% CL limits on Im c_d^γ and Im c_d^Z using $\mathcal{A}_{fb}$ and $\mathcal{A}_{ch}$ with unpolarized electron beam at cm energy 500 GeV and cut-off angle 35°. Mass of the top quark is taken to be (a) 174 GeV and (b) 200 GeV.

Fig. 2. Bands showing simultaneous 90% CL limits on Im c_d^γ and Im c_d^Z using $\mathcal{A}_{ch}$ with different beam polarizations, and at a cm energy of 500 GeV and cut-off angle 60°. Mass of the top quark is taken to be (a) 174 GeV and (b) 200 GeV.

Fig. 3. Bands showing simultaneous 90% CL limits on Im c_d^γ and Im c_d^Z using $\mathcal{A}_{fb}$ with different beam polarizations, and at a cm energy of 500 GeV and cut-off angle 10°. Mass of the top quark is taken to be (a) 174 GeV and (b) 200 GeV.

Table Captions

Table 1. Number of $t\bar{t}$ events, with either t or $\overline{t}$ decaying leptonically, for c.m. energy 500 GeV and integrated luminosity 10 fb^{-1} for two different top masses with polarized and unpolarized electron beams at different cut-off angles θ_0.

Table 2. Limits on dipole couplings obtainable from different asymmetries. In case (a) limits are obtained from $\mathcal{A}_{ch}$ and $\mathcal{A}_{fb}$ using unpolarized beams (Fig. 1), and in case (b) from either of $\mathcal{A}_{ch}$ (Fig. 2) and $\mathcal{A}_{fb}$ (Fig. 3) with polarizations $P_e = 0, \pm 0.5$. Charge-asymmetric angular distribution is used in case (c) where 0 and $\pm\, 0.5$ polarizations are considered separately. All the limits are at 90% CL.

	$m_t = 174$ GeV			$m_t = 200$ GeV		
θ_0	$P_e = -0.5$	$P_e = 0$	$P_e = +0.5$	$P_e = -0.5$	$P_e = 0$	$P_e = +0.5$
0°	1003	845	687	862	723	585
10°	988	832	675	849	712	576
35°	826	689	553	711	593	475
60°	507	419	330	438	362	286

Table 1

		$m_t = 174$ GeV		$m_t = 200$ GeV	
Case		$\|\mathrm{Im}c_d^\gamma\|$	$\|\mathrm{Im}c_d^Z\|$	$\|\mathrm{Im}c_d^\gamma\|$	$\|\mathrm{Im}c_d^Z\|$
(a) unpolarized		2.4	17	4.0	28
(b) polarized($P_e = 0, \pm 0.5$)		0.45	1.5	0.78	2.5
(c) angular distribution:	$P_e = +0.5$	0.13	0.74	0.21	1.21
	$P_e = 0.0$	0.13	0.81	0.20	1.30
	$P_e = -0.5$	0.12	0.28	0.18	0.43

Table 2

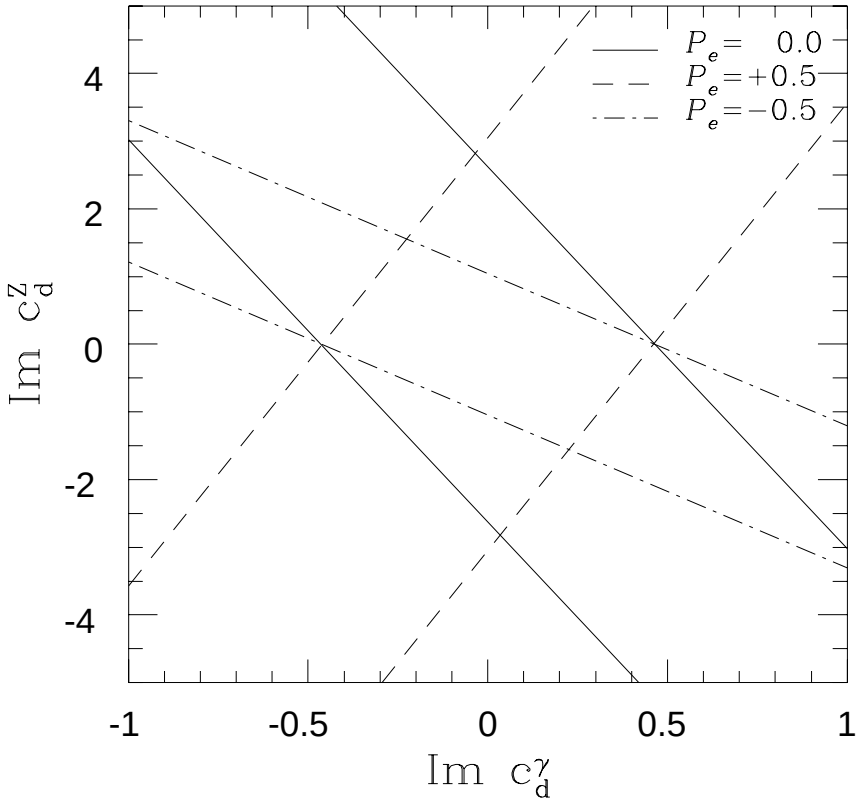
$P_e = 0.0$
$P_e = +0.5$
$P_e = -0.5$
4
2
0
-2
-4
-1
-0.5
0
0.5
1
Im c_d^Z
Im c_d^γ

Fig 2(a)

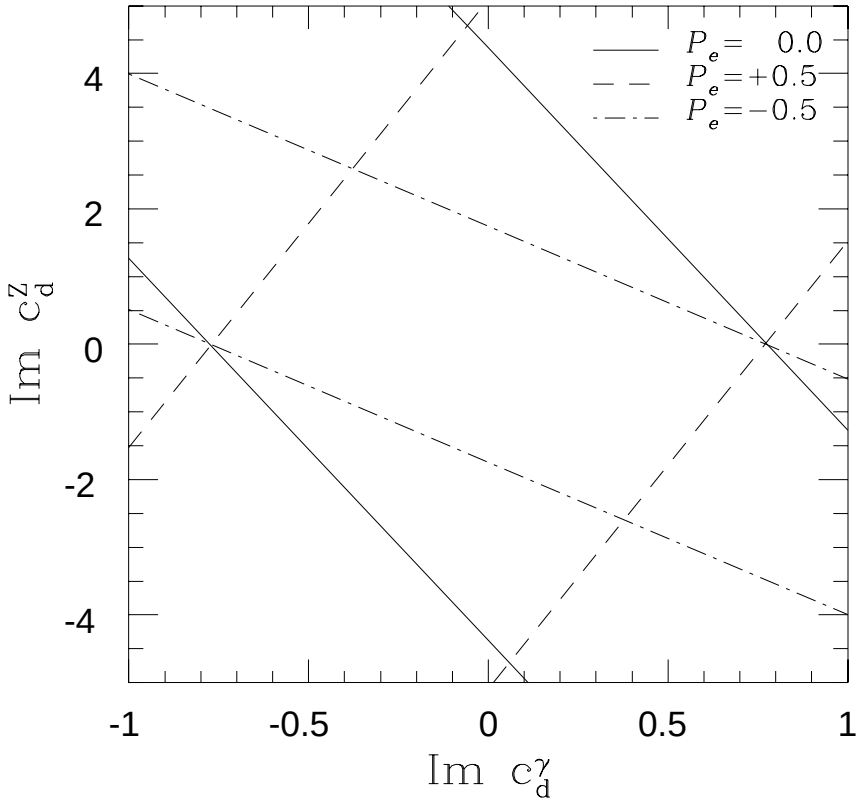
$P_e = 0.0$
$P_e = +0.5$
$P_e = -0.5$
4
2
0
-2
-4
-1
-0.5
0
0.5
1
Im c_d^Z
Im c_d^γ

Fig 2(b)

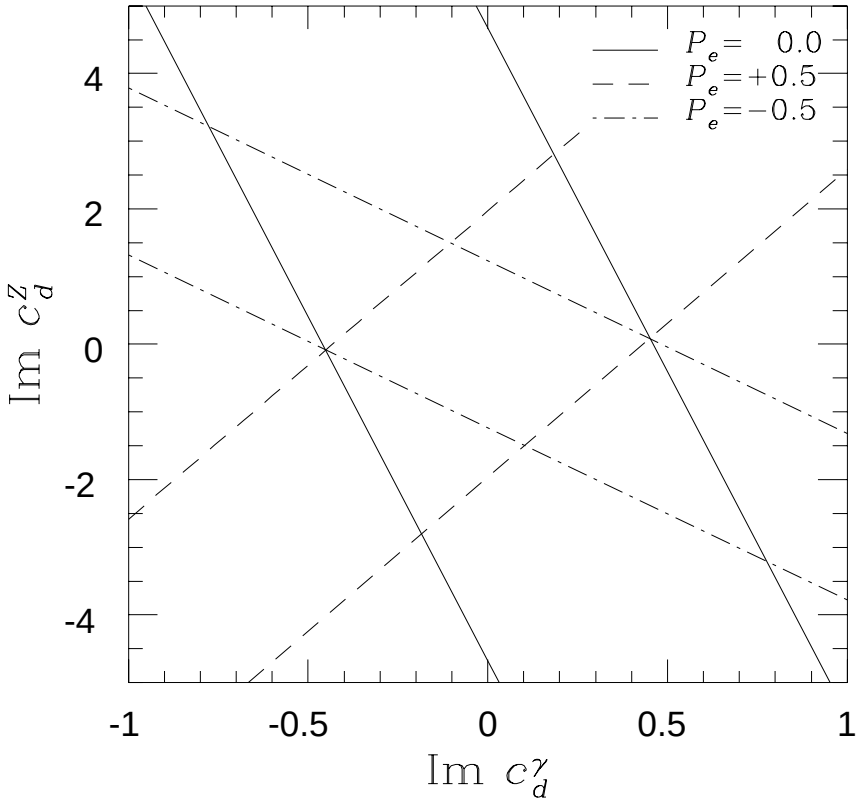
P_e= 0.0
P_e=+0.5
P_e=−0.5
4
2
0
-2
-4
-1
-0.5
0
0.5
1
Im c_d^Z
Im c_d^γ

Fig 3(a)

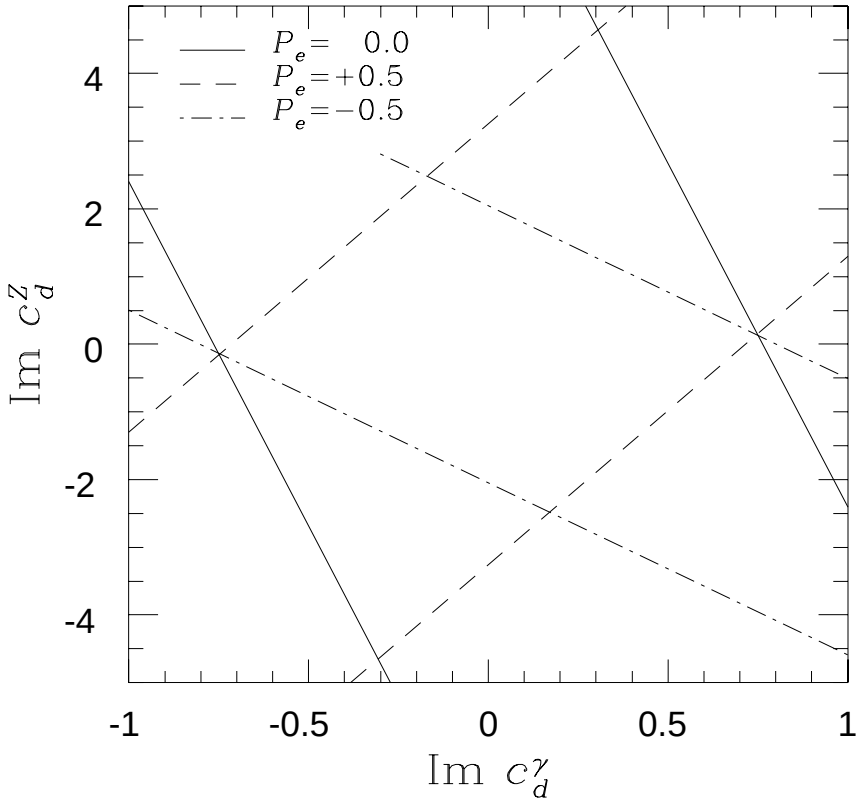
P_e= 0.0
P_e=+0.5
P_e=−0.5
4
2
0
-2
-4
-1
-0.5
0
0.5
1
Im c_d^Z
Im c_d^γ

Fig 3(b)

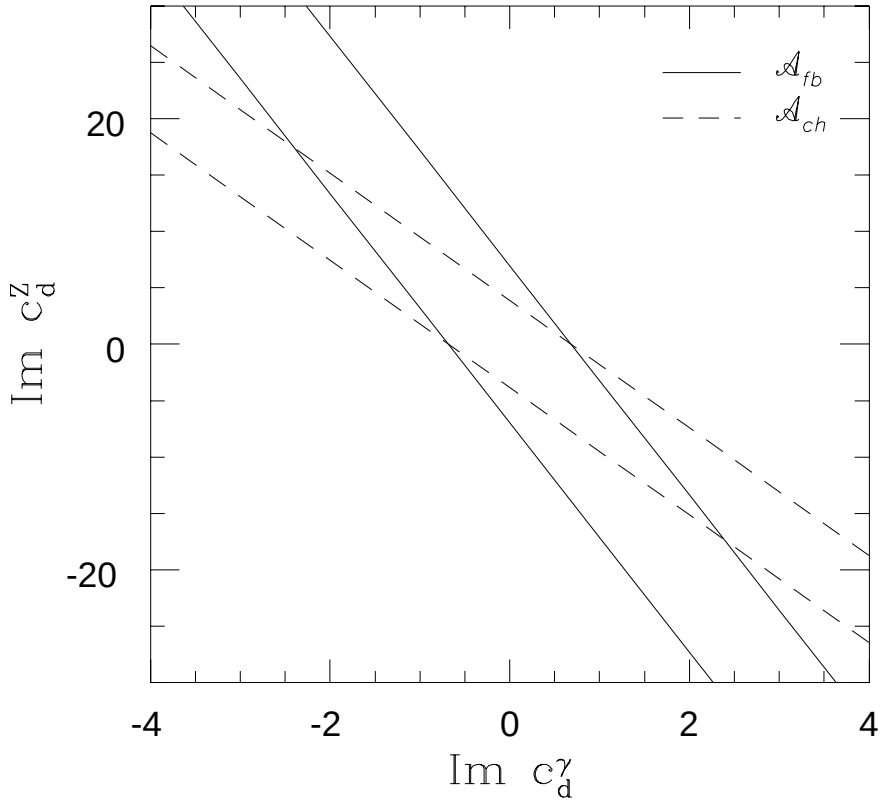
$\mathcal{A}_{fb}$
$\mathcal{A}_{ch}$
20
0
-20
-4
-2
0
2
4
Im c_d^Z
Im c_d^γ

Fig 1(a)

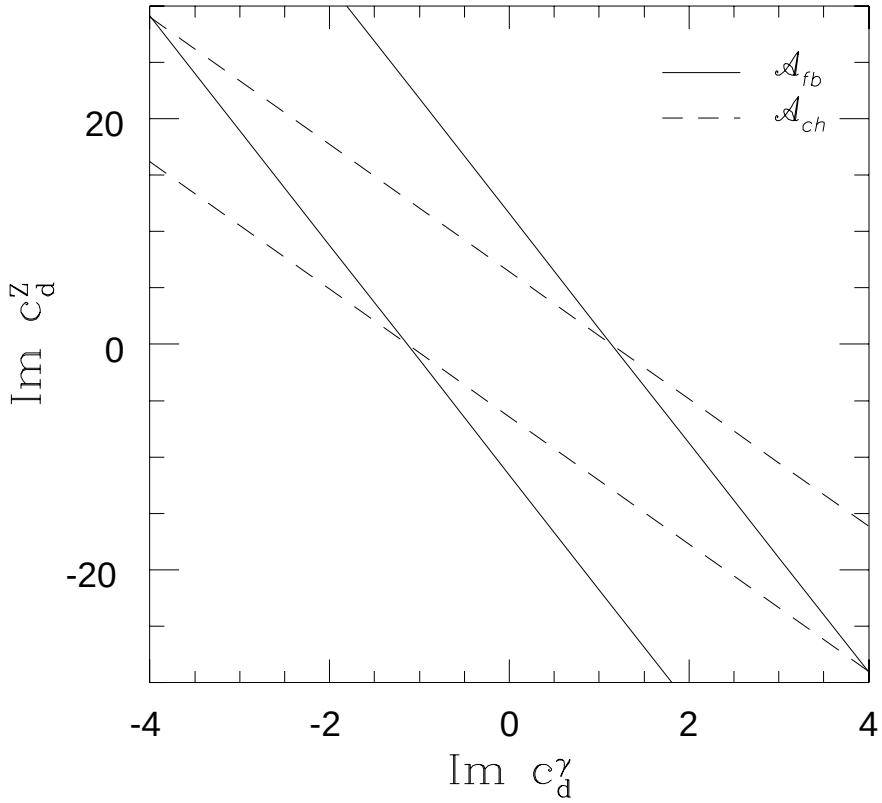
$\mathcal{A}_{fb}$
$\mathcal{A}_{ch}$
20
0
-20
-4
-2
0
2
4
Im c_d^Z
Im c_d^γ

Fig 1(b)